

## RESEARCH ARTICLE



## OPEN ACCESS

Received: 15-06-2022

Accepted: 04-10-2022

Published: 16-11-2022

**Citation:** Mani S, Nachiappan V (2022) Lack of Low-affinity Phosphate Transporter Pho91 Alters Lipid Metabolism in Yeast *Saccharomyces cerevisiae*. Indian Journal of Science and Technology 15(43): 2282-2289. <https://doi.org/10.17485/IJST/V15i43.1264>

\* **Corresponding author.**

\*[vasantinr@gmail.com](mailto:vasantinr@gmail.com)

**Funding:** University Research Fellowship provided by the Bharathidasan University, Trichy, India

**Competing Interests:** None

**Copyright:** © 2022 Mani & Nachiappan. This is an open access article distributed under the terms of the [Creative Commons Attribution License](https://creativecommons.org/licenses/by/4.0/), which permits unrestricted use, distribution, and reproduction in any medium, provided the original author and source are credited.

Published By Indian Society for Education and Environment ([iSee](https://www.indjst.org/))

**ISSN**

Print: 0974-6846

Electronic: 0974-5645

# Lack of Low-affinity Phosphate Transporter Pho91 Alters Lipid Metabolism in Yeast *Saccharomyces cerevisiae*

Subitha Mani<sup>1</sup>, Vasanthi Nachiappan<sup>1\*</sup>

<sup>1</sup> Bio-membrane Lab, Department of Biochemistry, School of Life Sciences, Bharathidasan University, Tiruchirappalli, 620024, Tamilnadu, India

## Abstract

**Objective:** The current study tries to elucidate the impact of low-affinity Pi transporter Pho91 (using *pho91Δ* cells) on lipid metabolism and cellular organelles morphology (mitochondria and vacuole) in yeast *Saccharomyces cerevisiae*. **Methods:** The lipid profile was performed using thin layer chromatography (TLC), and the membrane defect was determined using DiOC6 staining, lipid droplets (LDs) were observed by Nile red staining, mitochondrial morphology was observed using aconitase 1 GFP, vacuolar morphology was studied by FM4-64 staining and were performed with the aid of laser scanning fluorescent microscope. **Findings:** Pho91 is a low-affinity phosphate (Pi) transporter in the vacuoles that functions under Pi-rich conditions, but its role in lipid metabolism is largely unknown. In this study, we used defined synthetic complete media (SC). The deletion of Pho91 depicted a moderate growth defect but increased the major phospholipids PC, PE, and PI. Alterations in the membrane phospholipids resulted in defective membrane morphology. In *pho91* mutant (*pho91Δ*), the neutral lipids TAG and SE were increased and stored as LDs. The LD numbers were increased in *pho91Δ* cells than in WT cells. Altered phospholipids also defective mitochondrial morphology and enlarged vacuoles in *pho91* deletion. **Novelty:** In the absence of low-affinity Pi transporter *pho91*, it increases phospholipid, neutral lipid levels, LD numbers, and impacted mitochondria along with vacuolar structures.

**Keywords:** Phosphate transporter; Low affinity; Phospholipids; Neutral lipids; Lipid droplets

## 1 Introduction

Phosphorus as inorganic phosphate (Pi) is a vital macronutrient essential for the survival of living organisms. Pi is a component of various biomolecules responsible for the biosynthesis of phospholipids, DNA, RNA, and metabolites in energy metabolism. The inadequacy of intracellular Pi affects cell physiology, DNA replication, and phospholipid levels<sup>(1)</sup>. Phosphates are impenetrable to cellular membranes, integral membrane proteins are required to transport this essential macronutrient.

In budding yeast, these responses were controlled by a phosphate-responsive signaling (PHO) pathway called the PHO pathway. When cells are under Pi starvation, the transcription factors Pho4 and Pho2 get dephosphorylated and are translocated to the nucleus from the cytosol to induce the high-affinity Pi transporters, Pho84p and Pho89p to transport Pi from the extracellular to the intracellular environment to satisfy the Pi requirements; whereas low-affinity Pi transporters Pho87p, Pho90p and Pho91p function under Pi rich condition<sup>(2)</sup>.

Lipids are essential biomolecules of all eukaryotic organisms. Imbalance in lipid homeostasis is toxic to the cells<sup>(3)</sup>. Hence we studied the impact of *pho91Δ* cells on lipid levels. During Pi restriction, various genes are differently regulated, especially lipid phosphatase (Phm8), which is involved in the lipid metabolic pathway. It dephosphorylates lysophosphatidic acid (LPA), the storage lipids precursor for triacylglycerol (TAG). Phospholipids and neutral lipids are synthesized from LPA and PA precursors (phosphatidic acid)<sup>(1)</sup>.

Phospholipids can be synthesized by two metabolic pathways, CDP-DAG and Kennedy pathways. The most abundant phospholipids, phosphatidylcholine (PC) and phosphatidyl ethanolamine (PE) are part of the integral membrane components. With defined media, the phospholipids are mainly synthesized in the CDP-DAG pathway. The alternate Kennedy pathway is a salvage or subsidiary pathway that permits the synthesis of PC and PE when the primary CDP-DAG pathway is blocked. The PE is required for maintaining cell growth, metabolism of prokaryotes and eukaryotes, mitochondrial membrane integrity, and GPI anchor biosynthesis. Phosphatidyl serine (PS) is synthesized in the nuclear/ER membrane and is also required for the formation of phosphatidyl inositol (PI)<sup>(4)</sup>.

PA is dephosphorylated to diacylglycerol (DAG), and DAG is converted to TAG, a major storage lipid. The sterol ester (SE) is the second predominant neutral lipid (SE)<sup>(4)</sup>. Finally, LDs are specialized ubiquitous organelles containing the storage lipids surrounded by the phospholipid monolayer<sup>(5)</sup>.

Yeast vacuoles store the excess amount of Pi as polyphosphates (polyP). The polyP is a polymer of Pi residues up to a thousand linked through a phosphoric anhydride bond. When cells are starved of Pi, phospholipids, and stored polyP maintain Pi homeostasis<sup>(6)</sup>. The polyP is involved in proteostasis and acts as a protein chaperone against protein aggregation during Alzheimer's and Parkinson's diseases<sup>(7)</sup>. Pi and polyP levels inevitably play roles in cellular function and lipid metabolism. Hence, we focussed on *pho91*, a low-affinity Pi transporter located in the vacuoles and involved in the polyphosphate metabolism and regulates phosphate homeostasis and poly P levels<sup>(6)</sup>.

In our previous study, we used YPD (rich media – unknown amount of Pi) and observed the deletion of *pho91* alters lipid levels<sup>(1)</sup>. Here with SC medium (defined media - 7.35 mM of Pi), we studied the implications during the deletion of *pho91*, its impact on the lipid levels, and its effect on the structural aspect of mitochondria and vacuoles.

## 2 Methodology

*Saccharomyces cerevisiae*, BY4741 [MATa; his3Δ1; leu2Δ0; met15Δ0; ura3Δ0] and mutant strain *pho91Δ* were gifted by Prof. Ram Rajasekharan, Central Food Technological Research Institute, India who obtained the strains from Euroscarf (Frankfurt, Germany). The mutant strains used in this study are mentioned in Table 1. Synthetic Complete Media (SC) and thin layer silica gel plates were purchased from Difco and Merck. The lipid standards were purchased from Avanti Polar Lipids, Nile Red, ampicillin, solvents, and other chemicals were purchased from Sigma unless specifically mentioned.

**Table 1.** *Saccharomyces cerevisiae* strains used in this study

Strains / <i>Saccharomyces cerevisiae</i>	Relevant Characteristics	Source
BY4741	[MATa; his3Δ1; leu2Δ0; met15Δ0; ura3Δ0]	Prof. Ram Rajasekharan, CFTRI, India.
<i>pho91Δ</i>	[MATa; his3Δ1; leu2Δ0; met15Δ0; ura3Δ0; <i>pho91::kanMX4</i> ]	

### 2.1 Growth curve analysis/spot test

The *S. cerevisiae* wild-type strains (BY4741) and *pho91Δ* cells were grown in an SC medium at 30 °C until the mid-log phase. The cell density was adjusted to 1.0 OD at A600 nm. A series of 1:10, 1:100, 1:1000, and 1:10,000 dilutions were prepared, and three μl of each dilution was spotted on the SC media agar plate. Plates were incubated at 30 °C for 48 h, and growth was observed. The growth curve was analyzed by measuring cell growth in a UV-spectrophotometer OD (A<sub>600nm</sub>) at indicated time points until 48 h.

## 2.2 Lipid extraction and identification

The cells were grown in SC media until the mid-log phase, and the growth was measured ( $A_{600\text{ nm}}$ ), and equal numbers of cells (100 OD) were used for lipid extraction by Bligh and Dyer method<sup>(8)</sup>. Briefly, 400  $\mu\text{l}$  of chloroform and 200  $\mu\text{l}$  of methanol (2:1; v/v) were added to the cell pellet and vortexed, followed by 200  $\mu\text{l}$  of 2% orthophosphoric acid. The mix was vigorously vortexed and washed with PBS. The supernatant chloroform layer was dried and dissolved in 50  $\mu\text{l}$  of chloroform/methanol (2:1). Individual phospholipids were separated by two-dimensional thin-layer chromatography on silica gel plates using chloroform/methanol/25% $\text{NH}_3$  (65:25:5) as the solvent system for the first dimension and chloroform/acetone/methanol/acetic acid/water (50:10:25:15:5) as the solvent system for the second dimension. Phospholipids were visualized by staining with iodine vapor; the location of the individual lipids was compared with the  $R_f$  of the known standard. Spots corresponding to individual phospholipids were quantified<sup>(9,10)</sup>. For analyzing the neutral lipids, the chromatograms were developed in petroleum ether/diethyl ether/acetic acid (70:30:1) with triolein and cholesteryl oleate as standard, and the neutral lipids (TAG and SE) were quantified with slight modifications<sup>(11,12)</sup>. Briefly, we dipped the plates in methanolic  $\text{MnCl}_2$  staining solution (0.63 g  $\text{MnCl}_2 \cdot 4\text{H}_2\text{O}$ , 60 ml water, 60 ml methanol, and 4 ml concentrated sulfuric acid), dried, and heated at 120 °C for 15 min. Densitometric scanning was performed ( $A_{500\text{ nm}}$ ) with a CAMAG Scanner.

## 2.3 Nile red staining

Cells were grown in SC media up to the mid-log phase, the culture was centrifuged, and we washed the pellet with phosphate buffer saline (pH 8.0). Cells were fixed with 3.75% formaldehyde for 15 min and washed with an equal volume of PBS, then stained with lipophilic dye Nile red (20  $\mu\text{g}/\text{ml}$ ). Nile red-stained cells were washed with PBS and mounted on poly-lysine-coated slides that were sealed by the coverslips using nail polish. We obtained the fluorescence imaging with the help of a laser scanning fluorescent microscope (LSM 710-Zeiss) equipped with a 100x/1.40 oil objective and an AxioCam MRM camera. The experiment was performed using an excitation of 480 nm and an emission of 510 nm.

## 2.4 DiOC6 Staining (3, 3' dihexyloxocarbocyanine iodide)

WT, *pho91* $\Delta$  cells were grown in an SC media at 30 °C. Cells were harvested at the mid-log phase and washed with PBS, then stained the cell membrane using DiOC6, a lipophilic dye (1 mg/ml ethanol). After staining the cells, fluorescence imaging was performed on a confocal microscope (LSM 710-Zeiss) equipped with a 100/1.40 oil objective and an AxioCam MRM camera (Zeiss). The experiment was performed using an excitation of 488 nm and an emission of 520 nm.

## 2.5 Aconitase 1 GFP

WT, *pho91* $\Delta$  cells were grown in SC media containing 2% glucose along with 2% glycerol as respiratory control at 30 °C. Cells were harvested at the mid-log phase. Aconitase 1 GFP was overexpressed in WT, and *pho91* $\Delta$  were grown in SC media devoid of leucine (SC-Leu) at 180 rpm, 30 °C, then cells were harvested at mid-log phase, and cells were washed with PBS. Fluorescence imaging was performed on a confocal microscope (LS 710-Zeiss) equipped with a 100/1.40 oil objective and an AxioCam MRM camera (Zeiss) with excitation at 488nm 510nm for the emission wavelength.

## 2.6 FM4-64 Staining

The yeast vacuoles were stained with the lipophilic dye FM4-64 (Molecular Probes) according to the procedure reported earlier<sup>(13)</sup> with slight modification. The cells were grown in SC media containing 2% glucose at 30 °C with constant shaking. The cells were pelleted and resuspended with 500  $\mu\text{l}$  of fresh medium containing 20  $\mu\text{M}$  FM4-64 for 30 min, followed by washing with fresh medium and incubating with fresh medium for one h. The images were acquired on Zeiss LSM 700 confocal laser scanning microscope equipped with a 100X/1.40 oil objective and an AxioCam MRM camera (Zeiss) with 488 nm and 568 nm for excitation.

## 2.7 Statistical analysis

All the values reported in this work were the mean of three independent replicates. Statistical analysis was carried out by analysis of variance (ANOVA) test. Significant differences among mean were determined (\* $P < 0.05$ , \*\* $P < 0.01$ , and \*\*\* $P < 0.001$ ).

### 3 Results and Discussion

#### 3.1 Pho91 is required for the cell growth

Pho91 is an intracellular phosphate transporter that exports phosphate from the vacuole<sup>(6)</sup>. When we used YPD media, we observed growth rates in the *pho91Δ* cells and WT cells were similar. In the current study, we used SC media and studied the effect of cell growth in *pho91* deletion cells. The present study reveals with SC media, the deletion of *pho91* (low-affinity Pi transporter) slightly reduced cell growth than that with the WT cells (Figure 1).

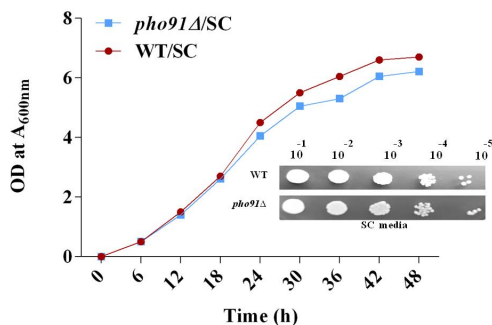


**Fig 1.** Growth study. WT, *pho91Δ* cells were grown in synthetic complete media (SC) at 30 °C, up to a mid-log phase, and the cells were harvested. The cells were serially diluted (10<sup>-1</sup> to 10<sup>-5</sup>), and 3 μl of cells were spotted on agar plates and incubated for 48 h at 30 °C. The growth curve was analyzed by measuring the cell’s OD (A<sub>600nm</sub>) at indicated time points until 48 h.

#### 3.2 Pho91 deletion cells increased Phospholipids

The impact of *pho91Δ* cells on lipid metabolism has not been studied in other labs, and we are the first to take up such a study. Earlier reports from our lab have been performed in various PHO deletion mutants (both high and low-affinity phosphate transporters) using the rich media with undefined Pi concentration. In the current study, we used defined SC media with defined Pi concentration. The PC and PE composition maintains the structural component of the cell membrane. We explored the impact on the membrane lipid homeostasis during the deletion of the low-affinity Pi transporter *pho91* (under SC media). Compared to the WT cells, the *pho91Δ* cells significantly increased the major phospholipids such as PC, PE, PI, and no significant changes were observed in PS and LPC (Figure 2). We observed no changes with PE and PI in YPD media.

The PI is predominantly present in the ER and is involved in ER membrane expansion<sup>(4)</sup>. PI levels were significantly increased in the *pho91Δ* cells. These results suggest that the deletion of *pho91* has an impact on membrane lipid homeostasis.

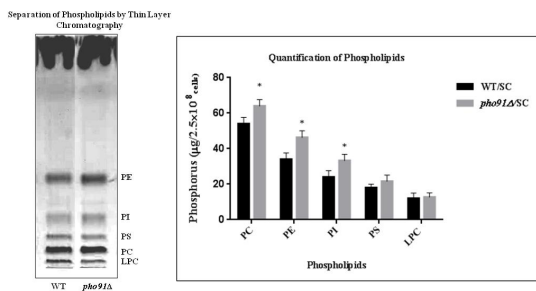


**Fig 2.** Quantification of Phospholipids. The WT and *pho91Δ* cells were grown in SC media up to a mid-log phase, cells harvested, and the lipids extracted and subjected to single–dimension TLC. The phospholipids were separated and quantified<sup>(10)</sup>.

### 3.3 Pho91 deletion causes defective membrane morphology

PC is a membrane phospholipid, a significant structural component for cellular membranes, and acts as a reservoir for several second messengers. PE is the second major phospholipid which is also required for cell membrane formation<sup>(14)</sup>. The significant phospholipids constitute 90% of total cellular phospholipids. The cells were stained with a lipophilic fluorescent dye DiOC6 to assess the intracellular membrane proliferation, and we observed a minor defect in the cellular membrane morphology with *pho91Δ* cells. The *pho91Δ* cells exhibited a strong green fluorescence all over the cells. In addition, they formed clumped aggregation (Figure 3), suggesting the plasma membrane is altered, which results in the accumulation of DiOC6 in the cytosol.

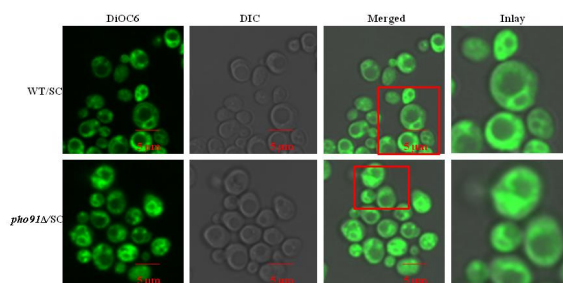


**Fig 3.** Membrane staining by DiOC6. The WT and *pho91Δ* cells were grown in SC media at 180 rpm, 30 °C. Cells were grown up to the mid-log phase, harvested, and washed with PBS, then the cells were stained using the lipophilic dye DiOC6. Fluorescence imaging was performed on a confocal microscope (LSM 710-Zeiss) equipped with a 100/1.40 oil objective and an AxioCam MRM camera (Zeiss) with excitation/emission at 488/520 nm.

### 3.4 The *pho91Δ* increases Neutral Lipids

In *S. cerevisiae*, PA is the precursor molecule for synthesizing phospholipids and neutral lipids<sup>(12)</sup>. The cells were grown in SC media, and when compared to the WT cells, deletion of Pho91 increased the neutral lipids (SE, TAG, and FFA levels), and sterol and DAG were marginally increased compared to WT cells (Figure 4). Compared to the previous studies with YPD media, the SC media depicted a distinct increase in SE, FFA, and sterol levels. The increased level of FFA and DAG leads to lipotoxicity and cell death<sup>(15)</sup>.

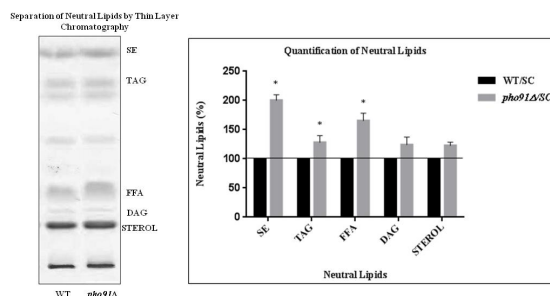


**Fig 4.** Quantification of neutral lipids. WT and *pho91Δ* cells were grown in SC media at 180 rpm, 30 °C, harvested at mid-log phase, extracted the lipids, and then subjected to TLC for neutral lipid separation. The individual neutral lipids were quantified by densitometry scanning.

In our previous study, the LD numbers were increased in *pho91* deletion with YPD. In the present study, also in the *pho91Δ* cells (in SC medium), the SE and TAG levels were increased to 200 and 140%, respectively. In addition, the phospholipid and neutral lipid levels were significantly increased. Triacylglycerol (TAG) and sterol esters (SE) are stored in the LDs, which are surrounded by phospholipid monolayer, and stored in a biologically inert form<sup>(16)</sup>. The LDs were stained using the lipophilic fluorescence Nile red, and an increased LD number was found in the *pho91Δ* cells than in WT cells grown with SC media (Figure 5).

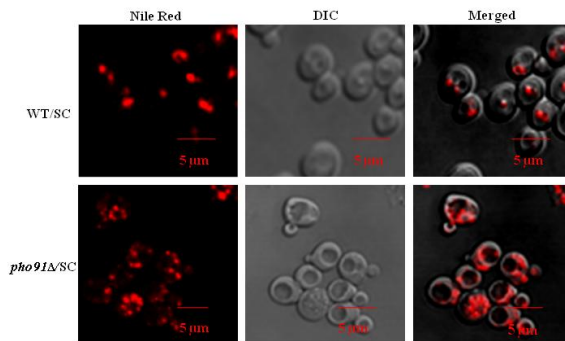


**Fig 5.** LD staining using Nile Red. The WT and *pho91Δ* cells were grown in SC media at 30 °C up to a mid-log phase. The cells were harvested, washed with PBS, and stained with the lipophilic fluorescence dye Nile Red. Fluorescence imaging was performed on a confocal microscope (LS 710-Zeiss) equipped with a 100/1.40 oil objective and an AxioCam MRM camera (Zeiss) with excitation and emission at 480 nm and 510 nm, respectively.

### 3.5 Deletion of Pho91 led to a defect in mitochondria

The lipids play a vital role in maintaining the membrane structure of the cellular organelles. PC and PE are the two significant phospholipids required to maintain the membrane morphology, including the mitochondria<sup>(17)</sup>. Deletion of *pho91* increased the PC and PE levels significantly more than in the WT cells. We studied the mitochondrial morphology of *pho91Δ* cells through confocal microscopy using aconitase 1 GFP along with 2% glycerol as respiratory control. The aconitase 1 GFP strongly binds to the mitochondrial membrane cells. The WT cells depicted a normal mitochondrial morphology, whereas a defective mitochondrial morphology was observed in the *pho91Δ* cells in both glucose and glycerol (Figure 6). In humans, dysfunction of mitochondria causes neurodegenerative diseases such as Huntington's disease (HD), Friedreich's ataxia (FRDA), amyotrophic lateral sclerosis (ALS)<sup>(18)</sup>. From the results, we found that *pho91* is required for normal mitochondrial morphology.

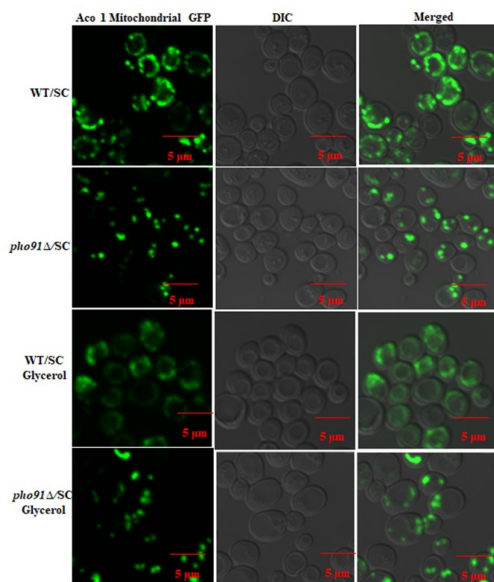


**Fig 6.** Confocal study for mitochondria by using Aconitase 1 GFP. Aconitase 1 GFP was overexpressed in WT, and *pho91Δ* were grown in SC media devoid of leucine (SC-Leu) at 180 rpm, 30 °C. Then cells were harvested at the mid-log phase and washed with PBS. Fluorescence imaging was performed on a confocal microscope (LS 710-Zeiss) equipped with a 100/1.40 oil objective and an AxioCam MRM camera (Zeiss) with excitation at 488nm 510nm for the emission wavelength.

### 3.6 Lack of Pho91 affects vacuolar morphology

*Saccharomyces cerevisiae* harbors for many evolutionary conserved proteins vacuolar protein localized in the vacuoles vacuolar morphology using the lipophilic dye FM4-64. The *pho91Δ* cells had an enlarged vacuolar structure (Figure 7).

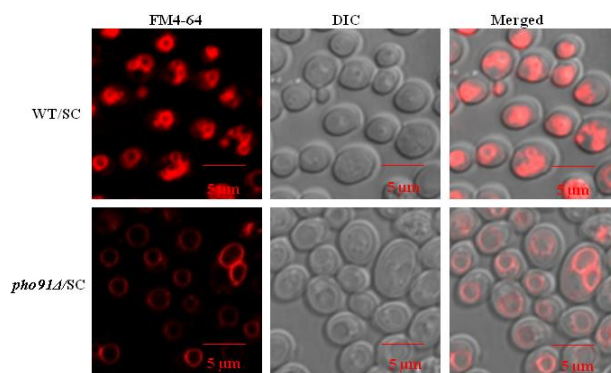


**Fig 7.** Confocal study for vacuoles using FM4-64 staining. The WT and *pho91Δ* cells were grown in SC media at 30 °C. The cells were harvested at the mid-log phase, and cells were washed with PBS and stained by FM4-64 stain. The fluorescence imaging was viewed on a confocal microscope (LS 710-Zeiss) equipped with a 100/1.40 oil objective and an AxioCam MRM camera (Zeiss) with 488/568 nm for excitation /emission.

## 4 Conclusion

The present result in SC media confirms the deletion of Pho91 induces mild cell growth defects. On the other hand, it shows a significant increase in the level of major phospholipids such as PC, PE, and PI. It also documented an increased TAG and SE, consequently leading to an increase in the number of lipid droplets in *Saccharomyces cerevisiae*. In addition to that, interestingly, we found that mitochondria and vacuolar morphology were affected in the deletion of *pho91*. Hence Pho91 is involved in the yeast lipid metabolism and is required for the normal cellular structure. To conclude, the Pi limitation could alleviate lipid metabolism, which causes the observed effects in *pho91Δ*. Furthermore, the mechanisms by which it is related to the violation of the transport of phosphate from the vacuoles by Pho91 would require further studies.

## Acknowledgment

The yeast strains were provided by Prof. Ram Rajasekharan, Central Food Technological Research Institute, India, and we gratefully acknowledge the same. We thank the UGC-BSR scheme for providing reagents for this study. University Research Fellowship provided by the Bharathidasan University, Trichy, India, is gratefully acknowledged. Instrumentation facilities offered by the Department of Biochemistry, Bharathidasan University, are gratefully acknowledged.

## References

- 1) Subitha M, James AW, Sivaprakasam C, Nachiappan V. Disruption in phosphate transport affects membrane lipid and lipid droplet homeostasis in *Saccharomyces cerevisiae*. *Journal of Bioenergetics and Biomembranes*. 2020;52(4):215–227. Available from: <https://doi.org/10.1007/s10863-020-09837-5>.
- 2) Tomashevsky A, Kulakovskaya E, Trilisenko L, Kulakovskiy IV, Kulakovskaya T, Fedorov A, et al. VTC4 Polyphosphate Polymerase Knockout Increases Stress Resistance of *Saccharomyces cerevisiae* Cells. *Biology*. 2021;10(6):487. Available from: <https://doi.org/10.3390/biology10060487>.
- 3) Csáky Z, Garaiová M, Kodedová M, Valachovič M, Sychrová H, Hapala I. Squalene lipotoxicity in a lipid droplet-less yeast mutant is linked to plasma membrane dysfunction. *Yeast*. 2020;37(1):45–62. Available from: <https://doi.org/10.1002/yea.3454>.
- 4) Kwiatek JM, Han GSS, Carman GM. Phosphatidate-mediated regulation of lipid synthesis at the nuclear/endoplasmic reticulum membrane. *Biochimica et Biophysica Acta (BBA) - Molecular and Cell Biology of Lipids*. 2020;1865(1):158434. Available from: <https://doi.org/10.1016/j.bbalip.2019.03.006>.
- 5) Robichaud S, Fairman G, Vijithakumar V, Mak E, Cook DP, Pelletier AR, et al. Identification of novel lipid droplet factors that regulate lipophagy and cholesterol efflux in macrophage foam cells. *Autophagy*. 2021;17(11):3671–3689. Available from: <https://doi.org/10.1080/15548627.2021.1886839>.
- 6) Austin S, Mayer A. Phosphate Homeostasis – A Vital Metabolic Equilibrium Maintained Through the INPHORS Signaling Pathway. *Frontiers in Microbiology*. 2020;11:1367. Available from: <https://doi.org/10.3389/fmicb.2020.01367>.
- 7) Sawada N, Ueno S, Takeda K. Regulation of inorganic polyphosphate is required for proper vacuolar proteolysis in fission yeast. *Journal of Biological Chemistry*. 2021;297(1):100891. Available from: <https://doi.org/10.1016/j.jbc.2021.100891>.
- 8) Bligh EG, Dyer WJ. A rapid method of total lipid extraction and purification. *Can J Biochem Physiol*. 1959;37(8):911–918. Available from: <https://doi.org/10.1139/o59-099>.

- 9) Siakotos AN, Rouser G, Fleischer S. Phospholipid composition of human, bovine and frog myelin isolated on a large scale from brain and spinal cord. *Lipids*. 1969;4(3):239–242. Available from: <https://doi.org/10.1007/BF02532639>.
- 10) Rouser G, Fleischer S, Yamamoto A. Two dimensional thin layer chromatographic separation of polar lipids and determination of phospholipids by phosphorus analysis of spots. *Lipids*. 1970;5(5):494–496. Available from: <https://doi.org/10.1007/BF02531316>.
- 11) James AW, Gowsalya R, Nachiappan V. Dolichyl pyrophosphate phosphatase-mediated N-glycosylation defect dysregulates lipid homeostasis in *Saccharomyces cerevisiae*. *Biochimica et Biophysica Acta (BBA) - Molecular and Cell Biology of Lipids*. 2016;1861(11):1705–1718. Available from: <https://doi.org/10.1016/j.bbali.2016.08.004>.
- 12) James AW, Ravi C, Srinivasan M, Nachiappan V. Crosstalk between protein N-glycosylation and lipid metabolism in *Saccharomyces cerevisiae*. *Sci Rep*. 2019;9(1):14485. Available from: <https://doi.org/10.1038/s41598-019-51054-7>.
- 13) Vida TA, Emr SD. A new vital stain for visualizing vacuolar membrane dynamics and endocytosis in yeast. *Journal of Cell Biology*. 1995;128(5):779–792. Available from: <https://doi.org/10.1083/jcb.128.5.779>.
- 14) Raj A, Nachiappan V. Hydroquinone exposure accumulates neutral lipid by the activation of CDP-DAG pathway in *Saccharomyces cerevisiae*. *Toxicology Research*. 2021;10(2):354–367.
- 15) Rockenfeller P, Gourlay CW. Lipotoxicity in yeast: a focus on plasma membrane signalling and membrane contact sites. *FEMS Yeast Research*. 2018;18(4):1–8. Available from: <https://doi.org/10.1093/femsyr/foy034>.
- 16) Bohnert M. New friends for seipin — Implications of seipin partner proteins in the life cycle of lipid droplets. *Seminars in Cell & Developmental Biology*. 2020;108:24–32. Available from: <https://doi.org/10.1016/j.semcdb.2020.04.012>.
- 17) Malina C, Larsson C, Nielsen J. Yeast mitochondria: an overview of mitochondrial biology and the potential of mitochondrial systems biology. *FEMS Yeast Research*. 2018;18(5):1–17. Available from: <https://doi.org/10.1093/femsyr/foy040>.
- 18) Wang Y, Xu E, Musich PR, Lin F. Mitochondrial dysfunction in neurodegenerative diseases and the potential countermeasure. *CNS Neuroscience & Therapeutics*. 2019;25(7):816–824. Available from: <https://doi.org/10.1111/cns.13116>.